SECURITY INFORMATION

CONFIDENTIAL

Copy 329
RM E53C02

NACA RM E53C02

NACA

RESEARCH MEMORANDUM

INVESTIGATION OF TURBINES FOR DRIVING SUPERSONIC COMPRESSORS

IV - DESIGN AND PERFORMANCE OF SECOND CONFIGURATION INCLUDING STUDY OF THREE-DIMENSIONAL FLOW EFFECTS

By Warren J. Whitney, Warner L. Stewart, and Harold J. Schum

Lewis Flight Propulsion Laboratory
Cleveland, Ohio

CLASSIFIED DOCUMENT

NATIONAL ADVISORY COMMITTEE FOR AERONAUTICS

WASHINGTON

May 18, 1953

CONFIDENTIAL

NATIONAL ADVISORY COMMITTEE FOR AERONAUTICS

RESEARCH MEMORANDUM

INVESTIGATION OF TURBINES FOR DRIVING SUPERSONIC COMPRESSORS

IV - DESIGN AND PERFORMANCE OF SECOND CONFIGURATION INCLUDING STUDY OF THREE-DIMENSIONAL FLOW EFFECTS

By Warren J. Whitney, Warner L. Stewart, and
Harold J. Schum

SUMMARY

The design and experimental performance are presented herein for a turbine configuration designed to drive a high-speed, high specific-weight-flow supersonic compressor. The design employed a concave inswept rotor hub contour and very little chordwise blade taper in order to alleviate the adverse three-dimensional flow problems that were encountered in a first configuration designed for the same application. Experimental results obtained with a 14-inch cold-air model of the turbine configuration under investigation indicated that satisfactory aerodynamic performance can be obtained in this application. The turbine passed design mass flow and extracted design specific work output at an efficiency of approximately 0.87 which was also the highest efficiency obtained. The results of radial surveys indicated that at design work extraction no part of the blade reached limiting loading, whereas in the first configuration limiting loading occurred before design specific work was obtained.

The experimental results presented herein, together with the pertinent experimental results obtained on the first configuration and the indications of a three-dimensional analysis which was made on both blade designs, are discussed to illustrate the applicability of an analysis of this type. Because of the agreement between the experimental results and the analytical indications, it was concluded that such a method should be incorporated into the design procedure of a turbine configuration wherever three-dimensional flow problems might be encountered.

INTRODUCTION

In many turbine applications, aerodynamic design requirements and limitations result in a turbine design in which the three-dimensional aspects of the flow are important. The results of an investigation of

a turbine configuration (referred to as the "first configuration") designed to power a high-speed, high-specific-weight-flow supersonic compressor indicated that it failed to meet design requirements (ref. 1); in subsequent investigations (refs. 2 and 3), it was determined that the poor performance was due to three-dimensional flow effects not considered in the design procedure. This turbine utilized a high degree of blade taper to reduce rotor-blade centrifugal stresses and a required increase in annulus area within the rotor was effected by means of a convex insweep of the inner wall. This type of insweep was used because of stress considerations.

In reference 4, a method of analyzing the effect of wall contouring and blade taper on the flow through a turbine is presented and applied to the rotor of reference 1. The analysis, which assumed axially symmetric flow, predicted that the rotor would choke at a weight flow considerably less than design and that the choking orthogonal would lie at the trailing edge at the rotor tip and well within the rotor at the hub. This location of the choking orthogonal indicated that the rotor tip would reach limiting loading considerably before the turbine limiting loading point (ref. 3). The two problems, weight flow and tip limiting loading, were experimentally verified in references 1 to 3. Hence, the method of analysis of reference 4, although approximate, proved satisfactory in indicating adverse three-dimensional flow effects.

The results of the analysis were also used to indicate modifications in the turbine design that would alleviate the adverse three-dimensional effects encountered. One possible modification would be a turbine configuration with a concave insweep of the rotor inner wall and little chordwise taper (ref. 4). This configuration would have the characteristics of the choking orthogonal meeting the inner wall at the lowest blade hub-tip ratio and lying near the trailing edge across the blade span. Hence, this configuration would be expected to have improved aerodynamic performance in comparison with the first configuration.

This report presents the design and experimental performance of the second turbine configuration, which was designed to power a supersonic compressor and which incorporated the modifications indicated in reference 3. The performance of this turbine is compared to that of the first configuration to show how proper consideration of the three-dimensional effects can result in the design of a satisfactory turbine. This investigation was conducted at the NACA Lewis laboratory.

SYMBOLS

The following symbols are used in this report:

A_{cr}/A	ratio of required area at Mach number of unity to required area at blade outlet Mach number
Δh	specific enthalpy drop, Btu/lb
M	Mach number
N	rotative speed, rpm
O	blade throat dimension, ft
p	absolute pressure, lb/sq ft
r	radius, ft
s	blade spacing, ft
$\Delta T'$	total-temperature drop, $^{\circ}R$
U	blade velocity, ft/sec
V	gas velocity, ft/sec
W	relative gas velocity, ft/sec
w	weight-flow rate, lb/sec
α	nozzle-outlet blade angle measured from tangential direction
γ	ratio of specific heats
δ	ratio of inlet-air total pressure to NACA standard sea-level pressure, p_1'/p^*
ϵ	function of γ, $\frac{\gamma^*}{\gamma}\left[\frac{\left(\frac{\gamma+1}{2}\right)^{\frac{\gamma}{\gamma-1}}}{\left(\frac{\gamma^*+1}{2}\right)^{\frac{\gamma^*}{\gamma^*-1}}}\right]$

η adiabatic efficiency defined as ratio of turbine work based on torque and weight-flow measurements to ideal turbine work based on inlet total temperature, and inlet and outlet total pressures, both defined as static pressure plus pressure corresponding to axial component of velocity

θ_{cr} squared ratio of critical velocity at turbine inlet to critical velocity at NACA standard sea-level temperature, $(V_{cr}/V^*_{cr})^2$

Subscripts:

1 measuring station upstream of nozzles

2 measuring station at nozzle outlet, rotor inlet

3 measuring station downstream of rotor

des design

r relative to rotor

t rotor tip or outer radius

Superscripts:

* NACA standard conditions

' total state

TURBINE DESIGN

Design Considerations and Requirements

The second turbine configuration was designed to drive the same compressor as the first configuration, which is described in reference 1. The compressor was assumed to develop a pressure ratio of 4 at an equivalent tip speed of 1372 feet per second and to handle an equivalent weight flow of 30 pounds per second per square foot frontal area. In order to alleviate the three-dimensional problems encountered in the first turbine configuration, the second configuration utilized little rotor axial taper and an axial inner wall at the rotor-blade outlet as discussed in reference 3.

The first turbine configuration was designed to accommodate liquid cooling (ref. 1). For the configuration investigated herein, it was assumed that air cooling would be used and that an internal taper would

have to be incorporated to reduce the rotor hub stress (e.g., see refs. 5 and 6) which, without any provision for stress reduction, would be on the order of 80,000 pounds per square inch. By using this cooling scheme, the external blade shape can be made nearly uniform in chord and thickness. An analysis of the cooling requirements for this turbine design was conducted and it was found that about 1 percent of the compressor weight flow was required. Thus, the design requirements for the cold-air turbine are changed slightly from those of reference 1 and are as follows:

$$\text{Equivalent weight flow, } \epsilon \frac{w\sqrt{\theta_{cr}}}{\delta} = 15.05 \text{ pounds per second}$$

$$\text{Equivalent tip speed, } \frac{U_t}{\sqrt{\theta_{cr}}} = 752 \text{ feet per second}$$

$$\text{Equivalent specific enthalpy drop, } \frac{\Delta h'}{\theta_{cr}} = 20.2 \text{ Btu per pound}$$

The equivalent performance requirements for the 14-inch turbine ($\gamma = 1.4$) were obtained from engine conditions ($\gamma = 1.3$) by the method of reference 7. The turbine design was based on the hot-gas conditions.

Design Procedure

Design velocity diagrams. - Velocity diagrams were constructed under the following assumptions:

(1) Free vortex flow

(2) Simple radial equilibrium

(3) Zero exit tangential velocity

(4) Isentropic flow through nozzles with a 0.95 percent flow coefficient

(5) Adiabatic efficiency of 0.92 was used to determine the rotor-blade throat areas

The velocity diagrams calculated on the basis of these assumptions are shown in figure 1(a). The diagrams are similar to those of reference 1, the slight changes being due to different design assumptions. The hub-tip radius ratios were 0.7 at the nozzle inlet and 0.61 at the

rotor outlet, the same as those of the configuration described in reference 1. However, the inner-wall contour of the nozzles and rotor blading was changed as suggested in reference 4. These changes effected an increasing annulus area in the nozzles; the increase continued in the rotor, reaching the maximum value at about 85 percent rotor axial chord, and the area remained constant thereafter.

A side view of the blading showing the inner wall curvature and the points where the velocity diagrams were calculated is presented in figure 1(b).

Rotor design. - Twenty-nine blades with solidities (based on chord) of 1.6 at the hub and 1.2 at the tip were used in the rotor design. The blade sections were laid out for the tip and for the section at 0.68 radius ratio to form smoothly converging channels. The sections were designed with a 2° angle of positive incidence. The rotor throat area and the blade exit angles were adjusted to maintain continuity between the throat and the outlet free-stream conditions, assuming no change in relative tangential velocity or additional losses between the two stations occurred. The blade was formed by positioning the two sections such that their centroids lay on a radial line and straight lines were faired between the two sections to connect points of equal percentage of surface between the leading and trailing edges. The resulting blade had approximately constant chord and had only a slight change in thickness from hub to tip. Figure 2 shows the two sections and table I presents the blade coordinates.

As part of the design procedure, a three-dimensional flow analysis was made to obtain the rotor choking weight flow; the method described in reference 4 was used for this analysis. The choking orthogonal for the second turbine is shown in figure 1(b). It was found that the choking orthogonal lies much closer to the trailing edge than that of the first turbine configuration (see ref. 4) and that, under isentropic conditions, 16.5 pounds air per second would be passed as compared with the design value of 15.05 pounds air per second. Hence, even with losses considered, no mass flow problem was indicated by the analysis.

Nozzle design. - As in reference 1, 32 nozzle blades were used, the mean solidity being 1.4. The design of the nozzle blades was based on the tip section and a section at 0.68 radius ratio. The required turning angle for these sections was 51° and 61°, respectively. The nozzle blades were designed with straight suction surfaces downstream of the throat and the throat dimension at the tip was obtained by the relation $O = s \sin \alpha$. At the hub, where the outlet Mach number was greater than unity, the equation was modified to $O = s \sin \alpha \, A_{cr}/A$.

The nozzle blade was formed by positioning the sections such that the centers of the trailing-edge radii lay on a radial line and straight lines were faired between the sections in the same manner as for the rotor blade. The nozzle blade sections are also shown in figure 2. As indicated previously, an insweep of the inner wall within the nozzle was utilized (see fig. 1).

APPARATUS, INSTRUMENTATION, AND PROCEDURE

The turbine used in this investigation was constructed in the same manner as that described in reference 1. Figure 3 shows a photograph of the rotor assembly. The apparatus, instrumentation, and methods of calculating the performance parameters are the same as those used in references 1, 3, and 4 with the exception of the measurement of the specific work output. The specific work output presented in this report was calculated by use of the weight-flow measurement and a torque measurement which was obtained from a strain-gage torquemeter similar to that described in reference 8.

For comparative purposes, the specific work output was also obtained by the temperature measurements as discussed in reference 3. It was found that around the design point the efficiencies as calculated by the two methods agreed to within 1 point. At off-design-operation conditions, a discrepancy occurred in which the torquemeter indicated somewhat lower efficiencies; it was felt that the specific work output as calculated by the torquemeter and weight-flow measurements was more accurate because it represented an integrated work output. Figure 4, which presents a diagrammatic sketch of the turbine rig, indicates the position of the torquemeter.

The turbine performance runs were made in the same manner as those of references 1, 3, and 4. The turbine-inlet temperature and pressure were maintained constant at nominal values of 135° F and 32 inches of mercury absolute, respectively. The speed was varied from 30 to 130 percent of design speed in even increments of 10 percent. At each speed, the total pressure ratio across the turbine was varied from the maximum possible (as dictated by the laboratory exhaust facilities) to approximately 1.40. Turbine adiabatic efficiency was based on the ratio of inlet total pressure to outlet total pressure (both defined as the sum of the static pressure and the pressure of the axial component of velocity, see ref. 1).

The absolute accuracy of the measured and calculated parameters is estimated to be within the following limits:

Temperature, °F	±0.5
Pressure, in. Hg	±0.05
Weight flow, percent	±1.0
Turbine speed, rpm	±20
Torque, percent design torque	±0.5
Efficiency, percent	±2.0

RESULTS

Turbine performance. - The over-all performance is presented in figure 5 with equivalent specific work $\Delta h'/\theta_{cr}$ shown as a function of the weight-flow speed parameter $\epsilon w N/\delta$, with total-pressure ratio p_1'/p_3' and efficiency η contours included. Design specific work was obtained at design speed at an efficiency of approximately 0.87 as represented by point A on the figure. As can be seen the design point occurs in a region of highest efficiency. Point B on the figure represents design specific work and design weight-flow parameter; a comparison of the abscissas of points A and B indicates that the turbine passed design weight flow.

The effect of turbine total-pressure ratio on the nozzle total-to-static pressure ratio at design speed is shown in figure 6. The total-to-static pressure ratios obtained from the design velocity diagram, in which simple radial equilibrium was assumed, are also included. At a total-pressure ratio corresponding to design specific work output, the nozzle total-to-static pressure ratio was very near the velocity diagram value at the outer wall but was considerably greater than the velocity diagram value at the inner wall. This discrepancy is believed to result from an additional pressure gradient which would occur in a radial-axial plane because of the convex curvature of the nozzle inner wall. The pressure-ratio curves indicate that, at design work output, the nozzle-outlet velocities were near the velocity-diagram values particularly at the tip section where the error resulting from the assumption of radial equilibrium would be a minimum. The trend of the pressure-ratio curves indicates that the rotor chokes at a turbine total-pressure ratio of about 2.1.

An indication of the radial blade element performance at design speeds can be obtained from figure 7, which presents the radial variation of total-temperature drop across the turbine for various total-pressure ratios. Since the turbine-outlet total temperature was measured in a fluctuating flow field, about 1 blade chord downstream of the rotor, the data must be considered only qualitative. However, the data are useful in comparing the general radial trends and the effect on the trends of total-pressure ratio.

It can be seen that at a total-pressure ratio of 2.06, which corresponds to design specific work output, there is no marked gradient in specific work output with radial position as was noted for the first turbine configuration (ref. 3). The trends with total-pressure ratio indicate that, at design specific work output, limiting loading had not occurred at any of the radial blade sections. The temperature-drop curves of figure 7 also indicate that limiting loading had not occurred at any blade section for a total-pressure ratio up to 2.26 which corresponds to a work output of 106 percent of design. The variation of the outer-shroud static pressure with axial position for several turbine total-pressure ratios at design speed is presented in figure 8. The static pressure at the blade outlet at the tip section is observed to decrease as the total-pressure ratio is increased beyond 2.06. This further indicates that, at design specific work output, the tip section has not reached limiting loading.

DISCUSSION

The approximate three-dimensional flow analysis method of reference 4 was applied to the subject turbine configuration and the results indicated that the blade passage would be able to pass the design weight flow. The location of the choking orthogonal as indicated by the analysis was nearer to the trailing edge at the hub section than it was in the first configuration (ref. 4); thus, the problem of tip limiting loading would be expected to be reduced. The experimental results presented herein verify both of these analytical results, as the subject turbine was found to be superior to the first turbine on the basis of passing the required weight flow, limiting loading at the blade tip, maximum efficiency obtained, and efficiency at design work output. It is therefore apparent that the effect of the three-dimensional flow characteristics must be considered in a turbine design to insure satisfactory turbine performance.

The results of the analysis of the first turbine configuration indicated that the aerodynamic problems of passing design mass flow and tip limiting loading would be encountered. An analysis of the second turbine configuration indicated that there would be no mass flow problem and that the tip limiting loading problem would either not be incurred or would be considerably alleviated. Since these performance characteristics predicted for both turbines were verified by experimental findings, this method of analysis can be considered to yield reliable indications although the method was approximate in that the assumptions of isentropic flow and axial symmetry were used.

SUMMARY OF RESULTS

The results of the investigation of a second turbine configuration designed to power a high-speed, high-specific-weight-flow compressor have indicated that inclusion of the three-dimensional flow effects in the turbine design resulted in satisfactory aerodynamic performance. By comparison, a first configuration that was designed for this application by a conventional technique which did not include the three-dimensional flow effects was found in a previous investigation to have unsatisfactory aerodynamic performance. Hence the second turbine configuration, with proper cooling and blade internal stress reduction, can be considered satisfactory for driving the high-speed, high-specific-weight-flow compressor.

The pertinent performance results of this second configuration can be summarized as follows:

1. At design speed, the turbine extracted design work output at an efficiency of approximately 0.87 which was the highest efficiency obtained.

2. At design speed and design work output, the turbine passed design weight flow.

3. As indicated by the total-temperature surveys at design speed, limiting loading had not occurred at any radial blade section for total-pressure ratios up to 2.26, which corresponded to a specific work output approximately 6 percent greater than design.

CONCLUSIONS

From the results of the investigation it can be concluded that the method of analysis, although approximate in that axial symmetry is assumed, gave an accurate indication of the important three-dimensional flow characteristics. Therefore, an analysis of the type used in this investigation should be used in a turbine design to indicate whether or not three-dimensional flow problems would be encountered. If the calculated adverse three-dimensional effects in the turbine design are avoided, satisfactory performance can result.

Lewis Flight Propulsion Laboratory
National Advisory Committee for Aeronautics
Cleveland, Ohio

REFERENCES

1. Stewart, Warner L., Schum, Harold J., and Whitney, Warren J.: Investigation of Turbines for Driving Supersonic Compressors. I - Design and Performance of First Configuration. NACA RM E52C25, 1952.

2. Stewart, Warner L., Schum, Harold J., and Wong, Robert Y.: Investigation of Turbines for Driving Supersonic Compressors. II - Performance of First Configuration with 2.2-Percent Reduction in Nozzle Flow Area. NACA RM E52E26, 1952.

3. Stewart, Warner L., Whitney, Warren J., and Monroe, Daniel E.: Investigation of Turbines for Driving Supersonic Compressors. III - First Configuration with Four Nozzle Settings and One Nozzle Modification. NACA RM E53A20, 1953.

4. Stewart, Warner L.: Analytical Investigation of Flow Through High-Speed Mixed-Flow Turbine. NACA RM E51H06, 1951.

5. Schramm, Wilson B., and Nachtigall, Alfred J.: Analysis of Coolant-Flow Requirements for an Improved, Internal-Strut-Supported, Air-Cooled Turbine-Rotor Blade. NACA RM E51L13, 1952.

6. Cochran, Reeves P., Stepka, Francis S., and Krasner, Morton H.: Experimental Investigation of Air-Cooled Turbine Blades in Turbojet Engine. XI - Internal-Strut-Supported Rotor Blade. NACA RM E52C21, 1952.

7. Heaton, Thomas R., Slivka, William R., and Westra, Leonard F.: Cold-Air Investigation of a Turbine with Nontwisted Rotor Blades Suitable for Air Cooling. NACA RM E52A25, 1952.

8. Rebeske, John J., Jr.: Investigation of a NACA High-Speed Strain-Gage Torquemeter. NACA TN 2003, 1950.

TABLE I - BLADE SECTION COORDINATES

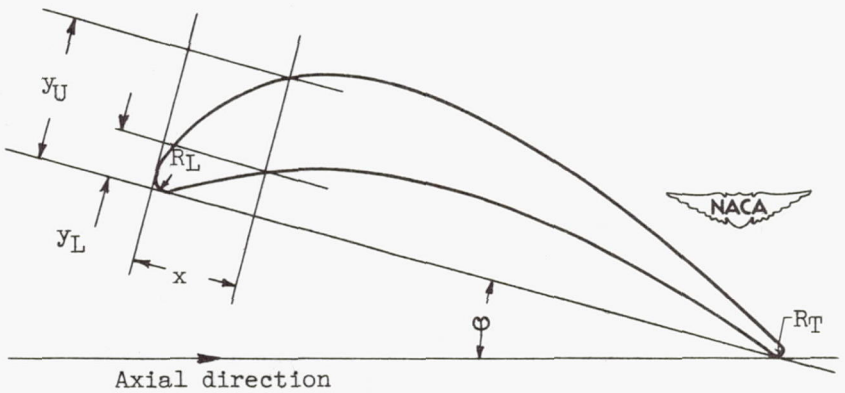

x	Nozzle				Rotor			
	Hub		Tip		Hub		Tip	
	y_L	y_U	y_L	y_U	y_L	y_U	y_L	y_U
0	0.075	0.075	0.075	0.075	0.050	0.050	0.050	0.050
.1		.197		.198	.025	.247	.008	.157
.2	.064	.258	.044	.265	.078	.350	.022	.216
.3	.115	.297	.081	.311	.104	.386	.036	.258
.4	.151	.317	.114	.337	.167	.454	.048	.285
.5	.173	.324	.142	.347	.197	.474	.060	.298
.6	.184	.319	.162	.349	.219	.481	.070	.300
.7	.185	.302	.174	.343	.233	.479	.078	.293
.794		.276						
.8	.177	(a)	.179	.329	.239	.469	.084	.278
.9	.164		.180	.307	.237	.452	.088	.260
.941				.296				
1.0	.147		.177	(a)	.229	.428	.089	.240
1.1	.126		.170		.214	.398	.086	.220
1.2	.102		.159		.195	.363	.081	.198
1.3	.076		.144		.172	.323	.072	.174
1.4	.048		.126		.145	.281	.061	.149
1.5	.018		.106		.114	.237	.047	.123
1.575	.015	.015						
1.6			.084		.081	.190	.031	.095
1.7			.061		.047	.139	.013	.066
1.793							.025	.025
1.8			.036		.013	.084		
1.873					.025	.025		
1.9			.010					
1.957			.015	.015				
φ	41.6°		34.7°		15.1°		32.9°	
R_L	0.075		0.075		0.050		0.050	
R_T	.015		.015		.025		.025	

[a]Straight-line fairing to trailing-edge circle.

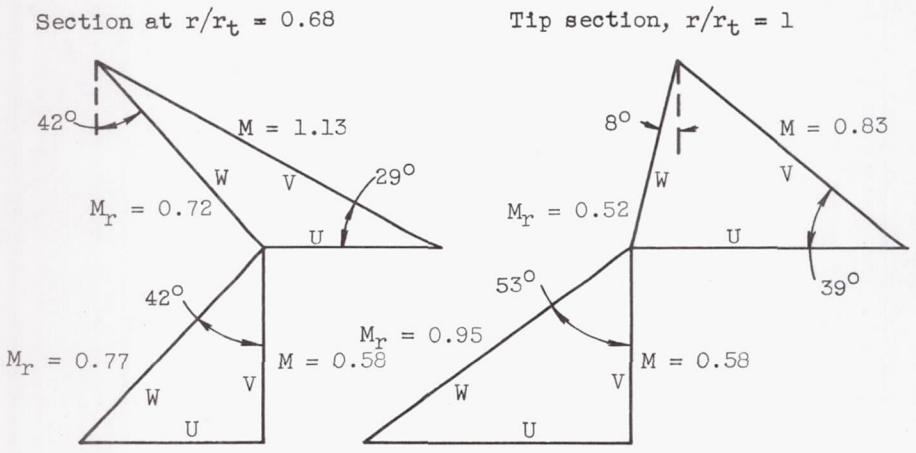

(a) Velocity diagrams.

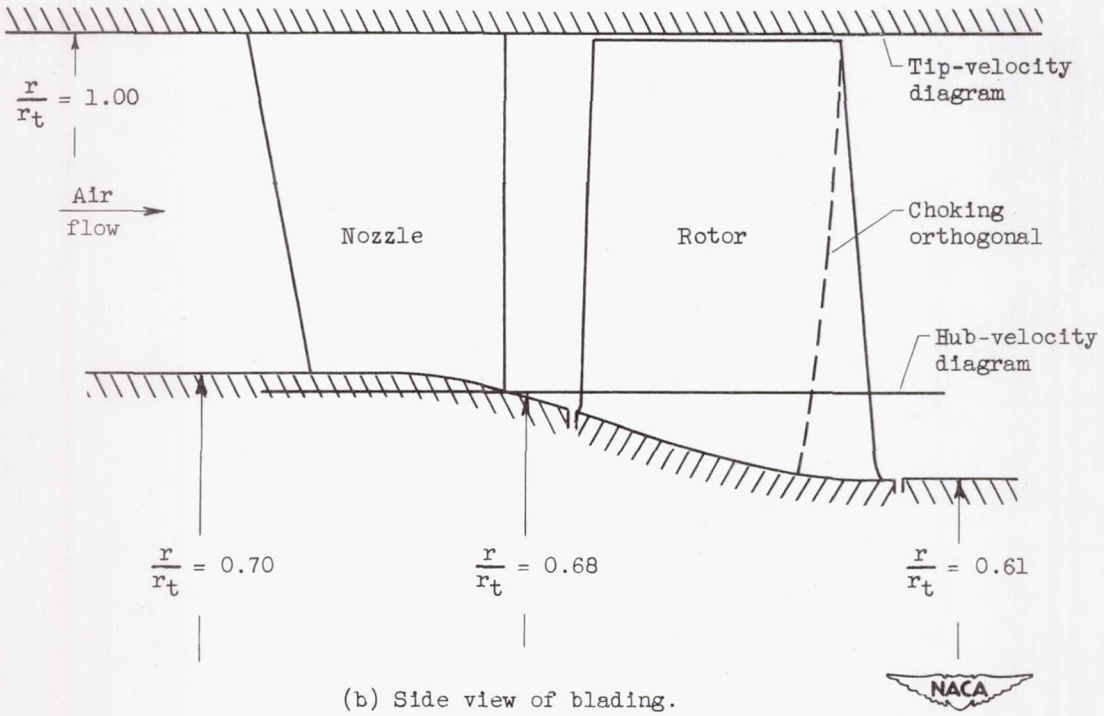

(b) Side view of blading.

Figure 1. - Design characteristics of turbine.

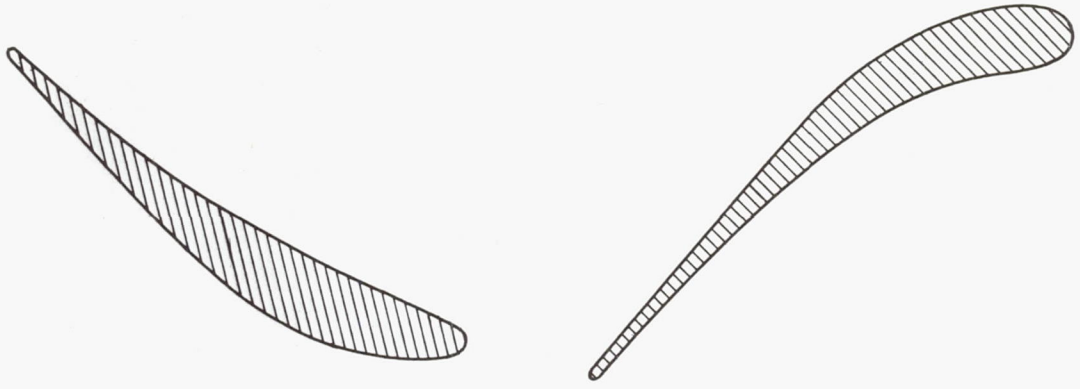

(a) Radius ratio, 1.00.

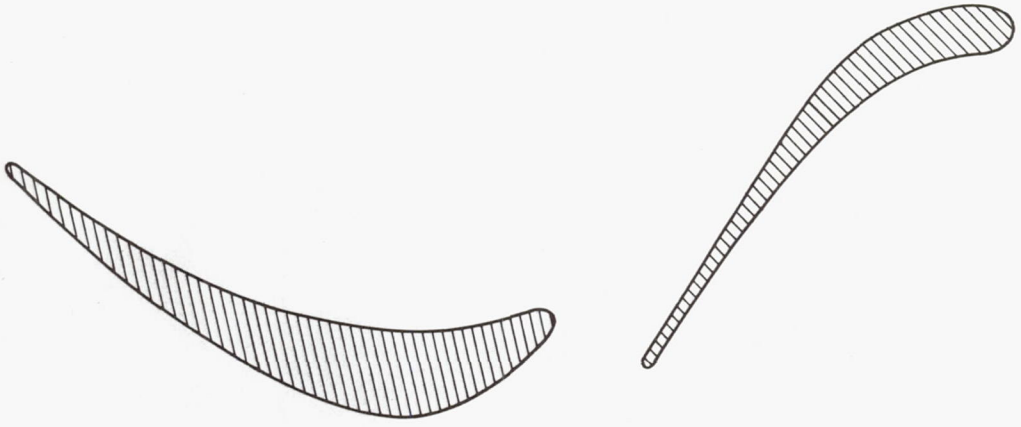

Rotor Nozzle

(b) Radius ratio, 0.68.

Figure 2. - Sketch of blade sections used in turbine design.

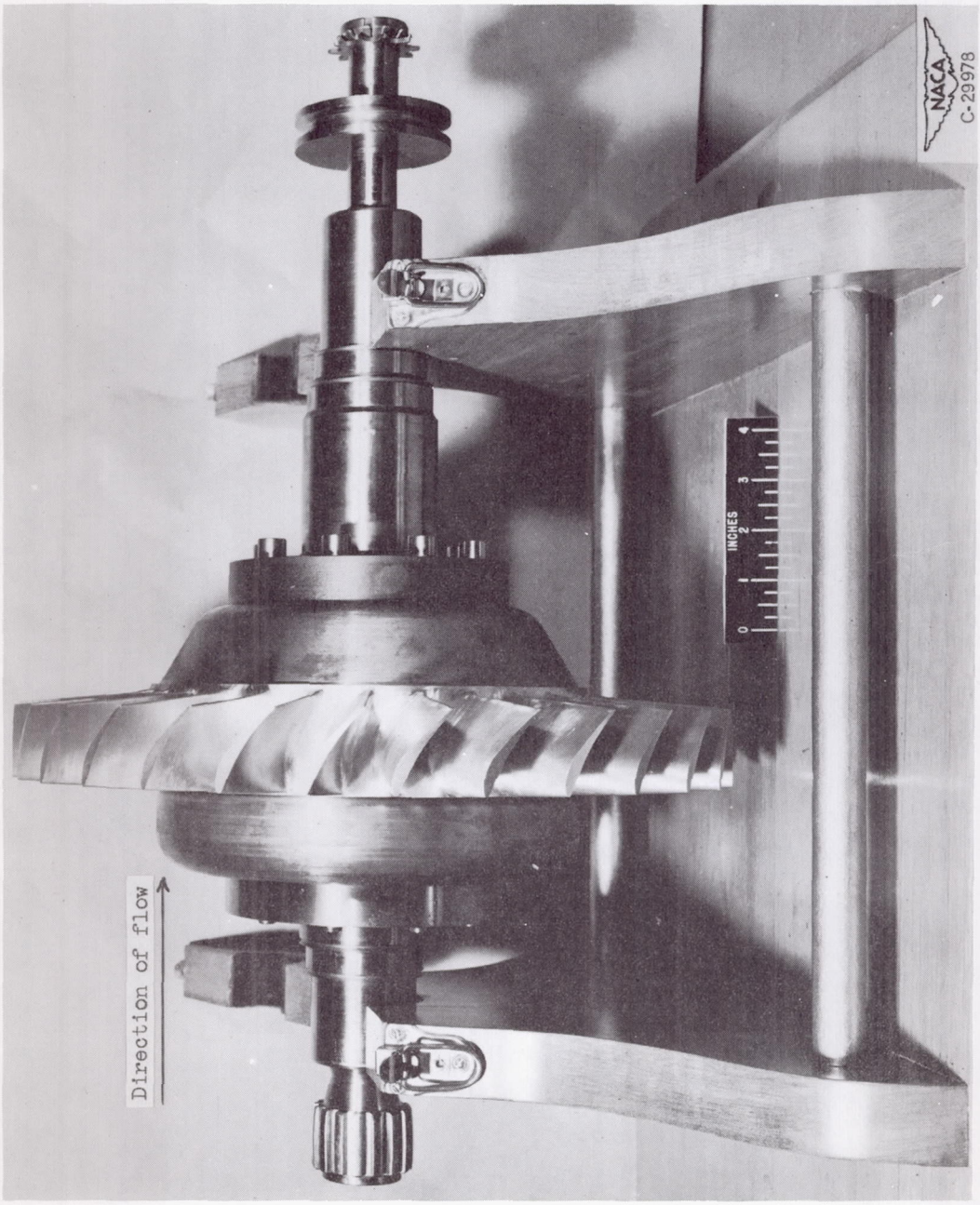

Figure 3. - Side view of turbine rotor assembly.

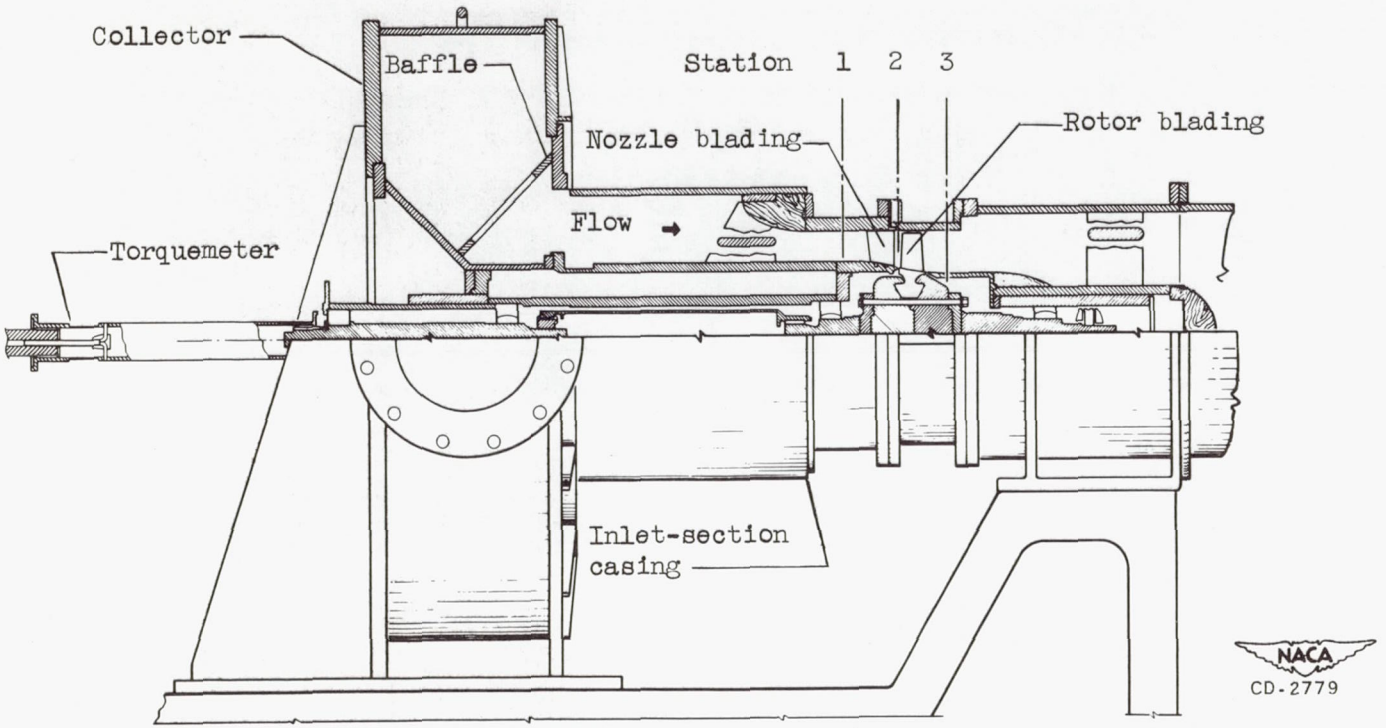

Figure 4. - Cold-air-turbine test section.

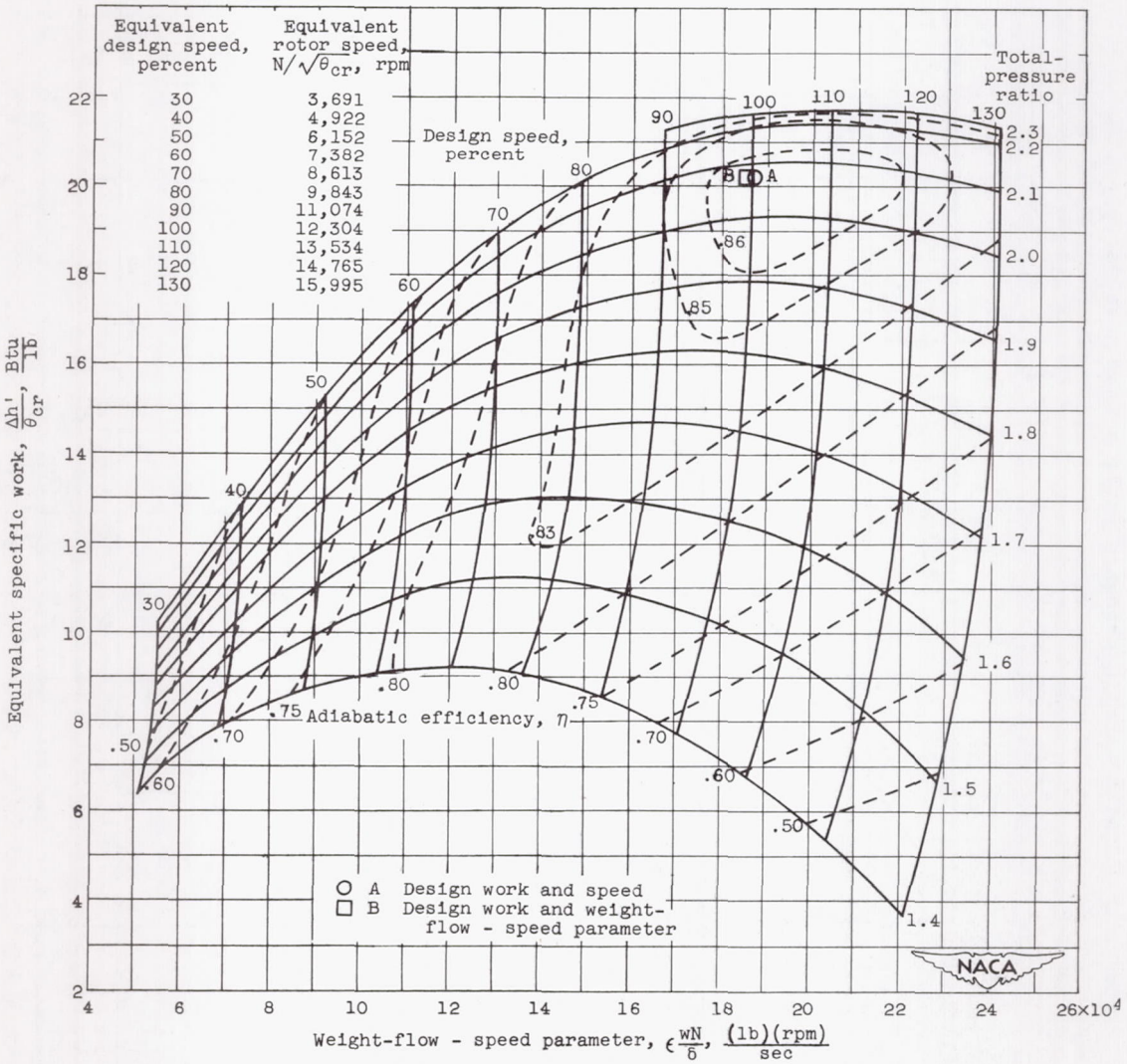

Figure 5. - Over-all performance of turbine.

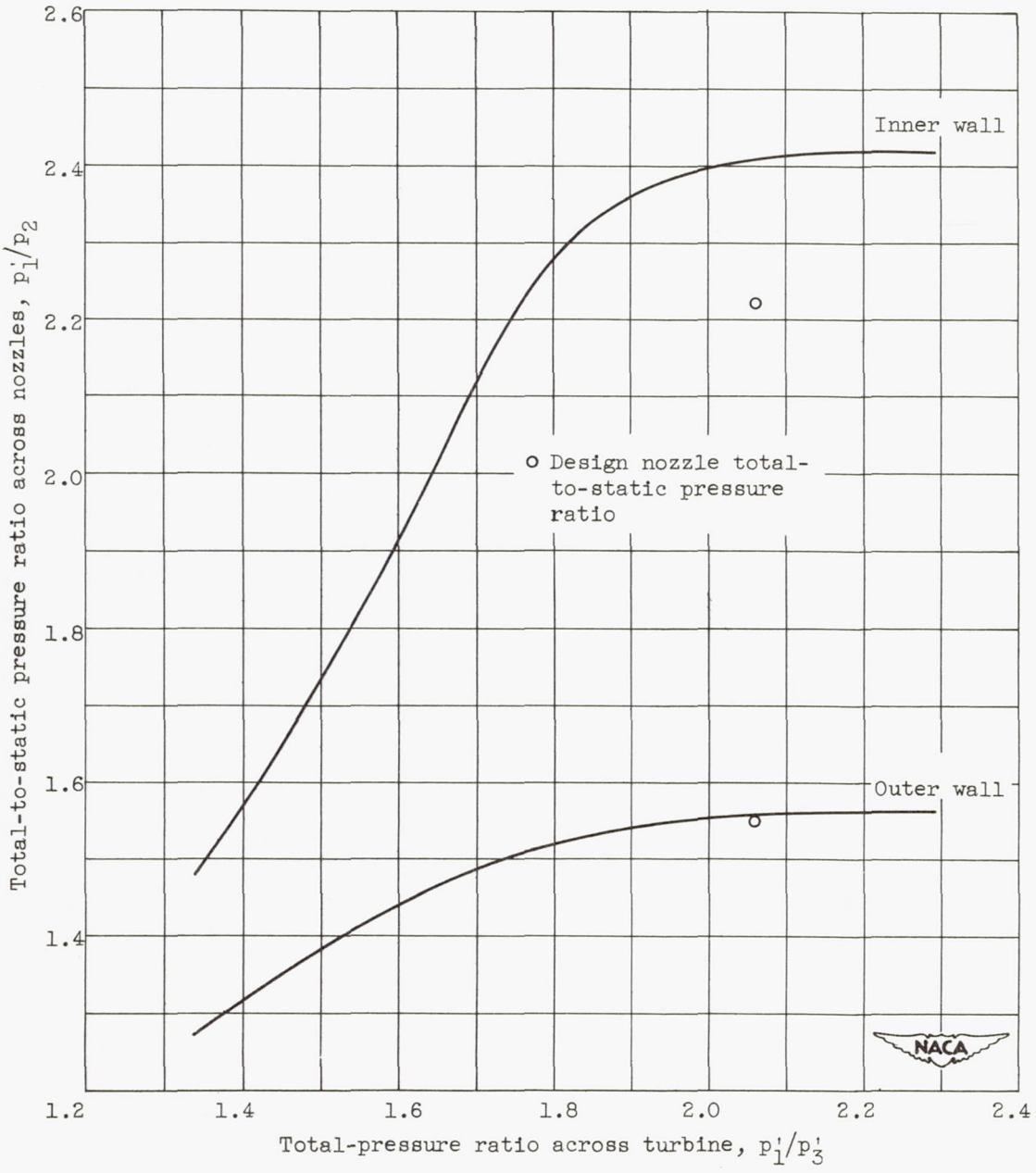

Figure 6. - Effect of total-pressure ratio across turbine on total-to-static pressure ratio across nozzle at design speed.

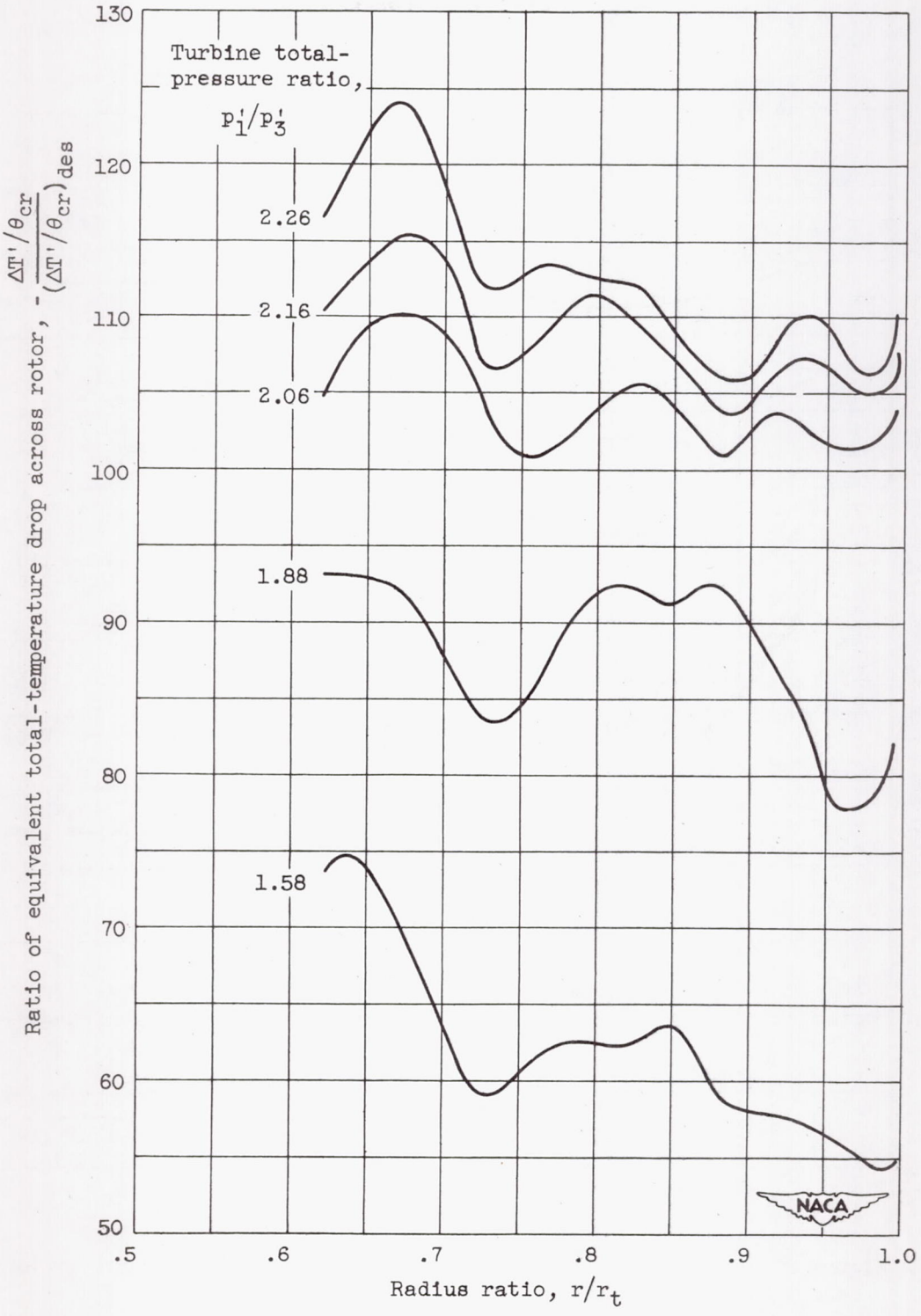

Figure 7. - Variation of equivalent total-temperature drop ratio with radius ratio at design speed for several total-pressure ratios.

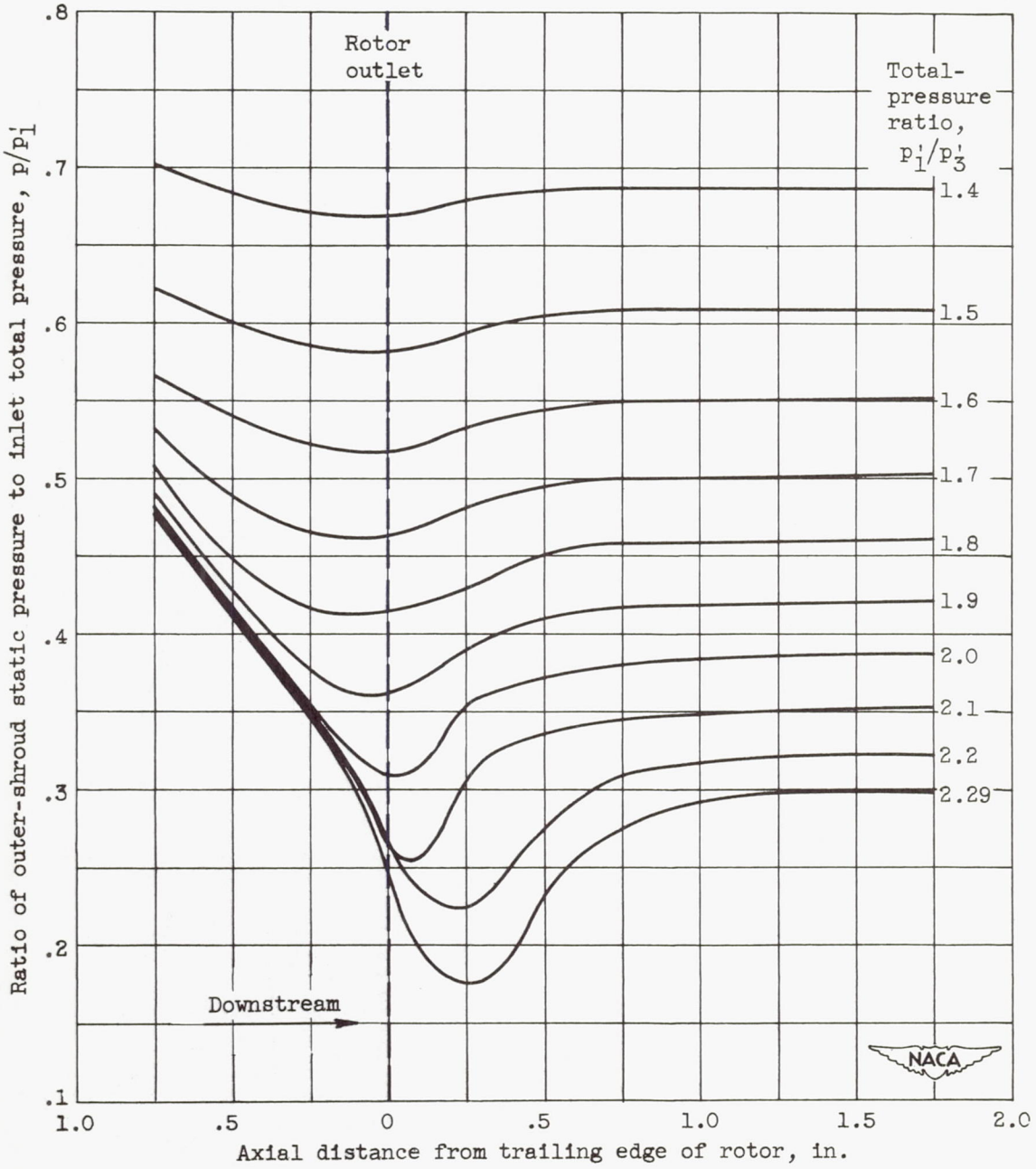

Figure 8. - Effect of total-pressure ratio on outer wall static pressure across rotor tip at design speed.

NACA-Langley - 5-18-53 - 400